

## Electrical Properties of Thermally Evaporated In<sub>40</sub> Se<sub>60</sub> Thin Films

Bushra A.Hasan, Ayat.M.Abdurazzaq  
University of Baghdad, College of Science, Department of Physics

---

**Abstract:** In<sub>40</sub> Se<sub>60</sub> thin films with different thicknesses (300,500, and 700nm) have been deposited by single source vacuum thermal evaporation onto glass substrates at ambient temperature to study the effect of thickness and on its structural morphology, and electrical properties. AFM study revealed that microstructure parameters such as crystallite size, and roughness found to depend upon deposition conditions. The DC conductivity of the vacuum evaporated In<sub>40</sub> Se<sub>60</sub> thin films was measured in the temperature range (293-473)K and was found to increase on order of magnitude with increase of thickness. The plot of conductivity with reciprocal temperature suggests, there are two activation energies E<sub>a1</sub> and E<sub>a2</sub> for In<sub>40</sub> Se<sub>60</sub> for all thicknesses which decreases with increasing thickness. Hall effect measurement showed that low thickness In<sub>40</sub> Se<sub>60</sub> film exhibit p-type conductance whereas the film exhibit n-type towards the higher thickness. The electric carrier concentration and mobility show opposite dependence upon thickness.

**Keywords:** In<sub>40</sub> Se<sub>60</sub> thin films, D.C, Hall effect.

---

### I. Introduction

Indium monoselenide (InSe) belongs to A<sup>III</sup>B<sup>VI</sup> layered semiconductor crystals [1]. It presents a layered structure, exhibiting weak -van der Waals\_ bonding between separate, covalently bonded Se-In-In-Se layers [1, 2]. Such layered crystal structure results in strong anisotropy of its properties [1]. InSe crystals can be easily cleaved along the basal plane. Atomically smooth surface of the cleaved facet features a low density of surface states ( $\leq 10^{10} \text{ cm}^{-2}$ ) and small value of root-mean-square roughness ( $\sim 0.05 \text{ nm}$ ) [3,4]. The absence of dangling bonds on InSe cleaved surface makes it possible to use this semiconductor as a substrate for growing molecular [5] and metal [6] nanostructures, as well as fabrication of heterostructures on the basis of semiconductor materials with different symmetries and lattice spacing [7-10]. The problem of the preparation of InSe high quality thin films is still unsolved due to the coexistence of several In-Se phases, that have been observed in films prepared by flash evaporation [11-15] vacuum evaporation [16-19] and by molecular beam epitaxy ~MBE [20-22].

### II. Experimental details

The compounds of In<sub>40</sub> Se<sub>60</sub> were prepared by quenching technique. The exact amount of high purity (99.999%) (In and Se) elements accordance with their atomic percentages were weighed using an electronic balance with the least count of ( $10^{-4} \text{ gm}$ ). The mixed elements were sealed in evacuated ( $\sim 10^{-3} \text{ Torr}$ ) quartz ampoule (length  $\sim 25 \text{ cm}$  and internal diameter  $\sim 8 \text{ mm}$ ). The ampoules which containing the elements were heated to 1073K at atmospheric pressure for 10 hours then cooled to room temperature. The temperature of the furnace was raised at a rate of  $10^\circ\text{C}/\text{min}$ . During heating the ampoules are constantly rocked. This is done to obtain homogeneous compounds. In<sub>40</sub> Se<sub>60</sub> thin of different thickness ( $t= 300, 500$  and  $700$ ) nm were prepared using thermal evaporation by continuously feeding the material with a powder to a heated molybdenum boat of melting point about 2895K at which temperature instantaneous evaporation of the material takes place.

Corning glass slides substrates were used, and the distance of the source to substrate was 15 cm. The evaporation carried out using Edward coating unit (model E306A). During the evaporation of the films, the pressure in the system was  $4 \times 10^{-5} \text{ Torr}$ . All the samples were prepared under constant condition [pressure, rate of deposition (3nm/sec), substrate temperature (room temperature). To study the electrical properties for the films Ohmic contacts for the prepared films are produced by evaporating (Al) electrodes of 300 nm thickness, by means of thermal evaporation methods. Then the d.c conductivity ( $\sigma$ ) has been studied using the electrical circuit which is consists of oven type Herease and Keithley (616). The thickness of the prepared films has been determined using Fizeau fringes of equal thickness are obtained in an optical aperture. The film thickness ( $t$ ) is

given by:  $t = \frac{\lambda \Delta x}{2 x}$  (1) Where  $\Delta x$  is the shift between the interference fringes,  $x$  is the distance between the

interference fringes and  $\lambda$  is the He: Ne wavelength (589.3 nm). The surface morphology of the In<sub>40</sub> Se<sub>60</sub> films were examined using AFM at room temperature. The structure dependent parameters, namely, crystallite size, roughness have been evaluated.

### III. Results and Discussion

Fig.1 shows three dimensional AFM images of In<sub>40</sub>Se<sub>60</sub> thin films grown with different thickness **300,500,700nm. Two-dimensional grain size of In<sub>40</sub>Se<sub>60</sub> thin films were measured by using nano scale reading.** It is obvious from table 1 that the average grain size get to increases with increase of thickness, indeed the grain size increases from 92 to 105 nm with increase of thickness from 300 to 700nm. Also the results showed that average roughness increases with thickness ,indeed average roughness increases from 0.68 to 0.83 nm when t increases from 300 to 700 nm .

Figure.2 represents the variation of conductivity versus inverse of absolute temperature with thicknesses for In<sub>40</sub>Se<sub>60</sub> films. It is observed that conductivity increases with increase in temperature .It is inferred that film material behaves as semi conducting at hole temperature range. For all the films, conductivity

follows the relation  $\sigma = \sigma_0 \exp\left(-\frac{E_a}{k_B T}\right)$  (2) where  $\sigma$  is conductivity at temperature T, and  $\sigma_0$  is the minimum

metallic conductivity (the value of  $\sigma$  when  $T \rightarrow \infty$ ),  $k_B$  is the Boltzmann constant and  $E_a$  is the activation energy. It is clear from these figures that there are two activation energy and hence two transport mechanism for In<sub>40</sub>Se<sub>60</sub> with different thickness. According to Davis and Mott model 1979[23] the tails of localized states should be rather narrow and extend a few length of tenths of an electron volt into the forbidden gap, and further more thus suggested of localized levels near the middle of the gap. This leads to three basically different channels of conduction:  $E_{a1}$  is the activation energy required to transport electron from Fermi level to the extended states above the conduction band edge  $E_c$ ,  $E_{a2}$  is the activation energy required to transport electron from Fermi level to the localized below the conduction band edge .

The increasing of thickness has no effect of the number on transport mechanisms of the system In<sub>40</sub>Se<sub>60</sub>. The variation of  $E_a$  for as -deposited In<sub>40</sub>Se<sub>60</sub> thin films with thickness and tin content are given in table 2. It is clear from this table that the activation energies decrease with the increase of film thickness. Indeed  $E_{a1}$  decreases from (0.0994to 0.00775) eV when the thickness increases from 300nm to 700nm, also  $E_{a2}$  decreases from (0.00955 to 0.00107) eV with the increase of thickness in the mentioned range. The decreasing of the activation energies with increasing of tin content may be due to the local ordering structure of the In<sub>40</sub>Se<sub>60</sub>. The decreasing of activation energy with the increase of thickness is resulting from the effect of reduction of energy gap and in turn reduces the energy requires to transport the carriers from Fermi level to the conduction band. The impurities, voids and defects present in the film are removed when thickness increased.

Hall effect phenomena is used as mentioned previously to determine the type of the majority charge carriers, concentration ( $n_H$ ) and Hall mobility ( $\mu_H$ ) for In<sub>40</sub>Se<sub>60</sub> thin films deposited at room temperature with different thicknesses (300, 500 and 700) nm . The coefficient of Hall ( $R_H$ ) were calculated and listed in table .3. It is clear from this table that the samples with thickness t=300 nm have a negative Hall coefficient (p-type), i.e. Hall voltage increases with the increase of the current, while for high thicknesses (t =700)nm the prepared samples reveal negative Hall coefficient (n-type charge carriers), i.e. Hall voltage decreases with the increase of the current. It is well established fact that In<sub>40</sub>Se<sub>60</sub> film exhibit p-type conductivity and this n-type conduction is generally attributed to free electrons from donor levels[24] . The density of this donor increases as thickness increases. Hence the increase in conductivity is probably due to decrease of energy gap of the film which is in good agreement with the earlier results reported in this paper.

### 3. Conclusions

There are three conduction mechanisms through out the D.C conductivity take place of In<sub>40</sub>Se<sub>60</sub> for low thickness. Increase of thickness improves the structure of the prepared thin films.

**Table.1 Average grain size and average roughness for In<sub>40</sub>Se<sub>60</sub> films with different thickness**

Thickness (nm)	Average grain size (nm)	Average roughness (nm)
300	92.98	0.682
500	102.44	0.534
700	105	0.836

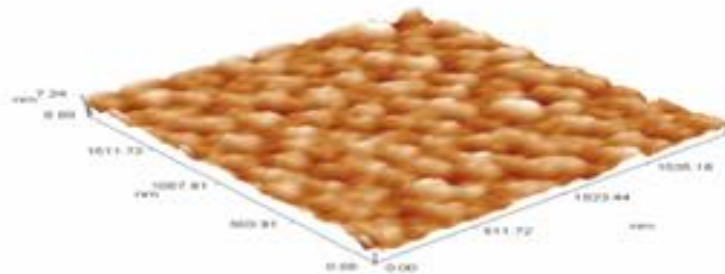
**Table.2 the values of E<sub>a1</sub>, and E<sub>a2</sub> and the temperature ranges for In<sub>40</sub>Se<sub>60</sub> films with different thickness.**

Thickness (nm)	E <sub>a2</sub> (eV)	Temp. Range (K)	E <sub>a1</sub> (eV)	Temp.Range (K)	$\sigma_{RT} * 10^{-5} (\Omega.cm)^{-1}$
300	0.00955	293-433	0.0994	433-473	0.916
500	0.00685	293-433	0.0416	433-473	2.01
700	0.00107	293-433	0.00775	433-473	7.25

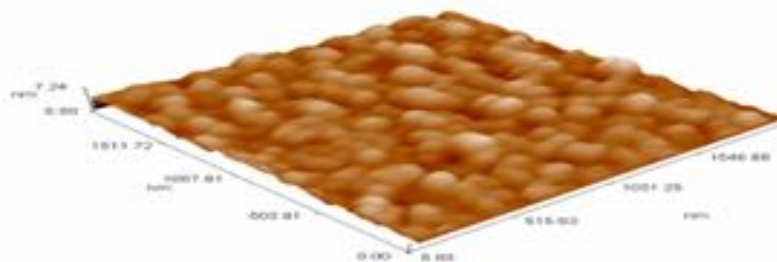
**Table.3 Hall Effect measurements for In<sub>40</sub>Se<sub>60</sub> film with different thicknesses.**

Thickness (nm)	$\sigma_{RT} (\Omega.cm)^{-1}$	R <sub>H</sub> (cm <sup>3</sup> /C)*10 <sup>8</sup>	n <sub>H</sub> (cm <sup>-3</sup> )	$\mu_H$ (cm <sup>2</sup> /V.sec)	type
300	1.3086E-05	3.1185	2.0645E+10	3369.16	p
500	1.0726E-05	0.214	0.34666E+10	137.31	p
700	1.4805E-05	-0.2070	1.1254E+12	1618.33	n

**t=300  
nm**



**t=500nm = 700nm**



$t=700nm$

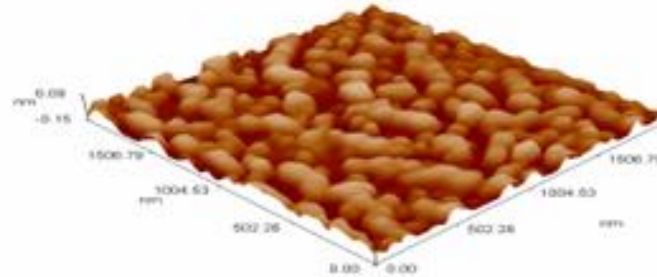


Fig. 1 AFM pictures for  $In_{40}Se_{60}$  films with different thickness.

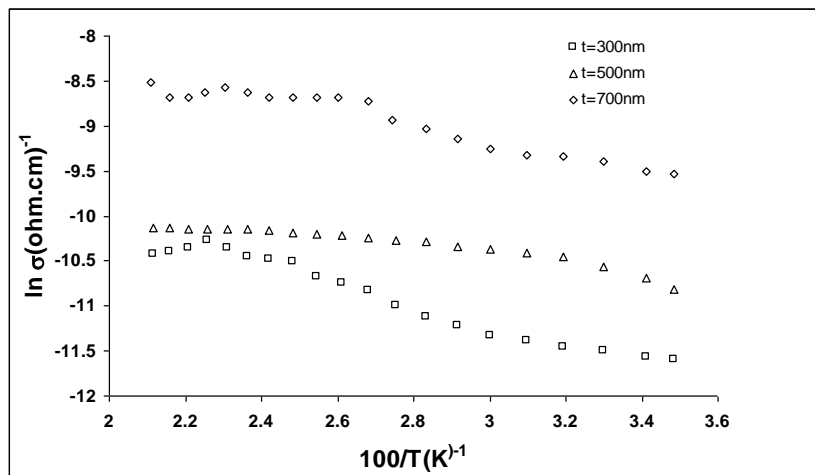


Fig. 4 the relation between  $\ln(\sigma)$  versus reciprocal of temperature for  $In_{40}Se_{60}$  films with different thicknesses.

### References

- [1]. F.S. Ohuchi, M.A. Olmstead, in: Wiley Encyclo-pedia of Electrical and Electronics Engineering, Ed.J.G. Webster, Wiley, New York 1999, Vol. 19, p. 147.
- [2]. I.C.I. Terhell, Prog. Cryst. Growth Charact. 7, 55(1983).
- [3]. V.M. Katerynychuk, Z.D. Kovalyuk, Semicond. Phys.Quantum Electron. Optoelectron. 14, 106 (2011).
- [4]. V.M. Katerynychuk, Z.D. Kovalyuk, Inorg. Mater.47, 749 (2011).
- [5]. K. Ueno, K. Sasaki, K. Saiki, A. Koma, Jpn. J. Appl.Phys. 38, 511 (1999).
- [6]. W. Jaegermann, C. Pettenkofer, B.A. Parkinson, Phys. Rev. B 42, 7487 (1990).
- [7]. N. Wisotzki, A. Klein, W. Jaegermann, Thin Solid Films 380, 263 (2000).
- [8]. A.P. Bakhtinov, V.N. Vodop'yanov, E.I. Slyn'ko,Z.D. Kovalyuk, O.S. Lytvyn, Tech. Phys. Lett. 33,86 (2007).
- [9]. V.M. Katerynychuk, Z.R. Kudrynskyi, Z.D. Kovalyuk,J. Nano-Electron. Phys. 4, 02042 (2012).
- [10]. Z.D. Kovalyuk, V.M. Katerynychuk, A.I. Savchuk,O.M. Sydor, Mater. Sci. Eng. B 109, 252 (2004).
- [11]. J. P. Guesdon, C. Julien, M. Balkanski, and A. Chevy, Phys. Status SolidiA **101**, 495 ~1987!.
- [12]. J. P. Guesdon, B. Bobbi, C. Julien, and M. Balkanski, Phys. Status SolidiA **102**, 327 ~1987!.
- [13]. C. Julien, N. Benramdane, and J. P. Guesdon, Semicond. Sci. Technol. **5**, 905 ~1990!.
- [14]. N. Benramdane, J. P. Guesdon, and C. Julien, Phys. Status Solidi A **146**, 675 ~1994!.
- [15]. C. Julien, A. Khelfa, N. Benramdane, and J. P. Guesdon, J. Mater. Sci. **30**, 4890 ~1995!.
- [16]. S. K. Biswas, S. Chaudhuri, and A. Choudhury, Phys. Status Solidi A **105**, 467 ~1988!.
- [17]. B. Thomas and T. R. N. Kutty, Phys. Status Solidi A **119**, 127 ~1990!.
- [18]. Y. Igasaki, H. Yamauchi, and S. Okamura, J. Cryst. Growth **112**, 797 ~1991!.
- [19]. S. Marsillac, J. C. Berne' de, and A. Conan, J. Mater. Sci. **31**, 581 ~1996!.
- [20]. J. Y. Emery, C. Julien, M. Jouanne, and M. Balkanski, Appl. Surf. Sci. **33,34**, 619 ~1988!.
- [21]. J. Y. Emery, L. Brahim-Otsmane, C. Herlemann, and A. Chevy, J. Appl. Phys. **71**, 3256 ~1992!.
- [22]. L. Brahim-Otsmane, J. Y. Emery, and M. Eddrief, Thin Solid Films **237**, 291 ~1994!.
- [23]. N. Mott. and E. Davis'Electronic Process in Non-crystalline Materials', 2<sup>nd</sup> ed., University Press, Oxford P.858 (1979).
- [24]. S. M. Sze, Physics of semiconductor Devices, Wiley,New York, 1981,849 and 751.